Spike Sorting based on Dominant-Sets clustering

D. A. Adamos[1], N. A. Laskaris[2], E. K. Kosmidis[3] and G. Theophilidis[1]

[1] Laboratory of Animal Physiology, School of Biology, Aristotle University of Thessaloniki (AUTh), 54 124, Greece
[2] Laboratory of Artificial Intelligence & Information Analysis, Department of Informatics, AUTh, 54 124, Greece
[3] Laboratory of Physiology, School of Medicine, AUTh, 54 124, Greece

Abstract—**Spike sorting algorithms aim at decomposing complex extracellularly recorded electrical signals to independent events from single neurons in the vicinity of electrode. The decision about the actual number of active neurons in a neural recording is still an open issue, with sparsely firing neurons and background activity the most influencing factors. We introduce a graph-theoretical algorithmic procedure that successfully resolves this issue. Dimensionality reduction coupled with a modern, efficient and progressively-executable clustering routine proved to achieve higher performance standards than popular spike sorting methods. Our method is validated extensively using simulated data for different levels of SNR.**

Keywords— **Spike sorting, dominant sets, graph-theoretic clustering, ISOMAP, manifold learning**

I. Introduction

The basis of every spike sorting algorithm is the assumption that all the action potential traces of a particular neuron have nearly the same amplitude and shape. In extracellular recordings, the shapes of recorded spike waveforms mainly depend on neuron's geometry as well as its distance to the recording electrode. The goal of a spike sorting routine is to process and analyze the usually composite recorded signals in order to identify the number of active neurons and extract detailed time courses of their spiking activity. Related algorithms constitute the core methodological component in various situations ranging from traditional neurophysiological experiments and clinical/neuroscience studies to cortex-machine interfaces.

The battery of available spike sorting routines includes mainly automated techniques that analyze the recorded signals by means of their waveforms. At the initial stage, various linear techniques like Principal Component Analysis (PCA) and wavelets are used in order to reduce the dimensionality of the input data and enhance the signal content in the attempted representation. PCA-based projection is often restrained within the subspace spanned by the first two or three principal components, although the employment of more components has recently been reported to carry useful complementary information [1]. Alternatively, the wavelet transform is used for the decomposition of spike waveforms [2], featuring improved discrimination of localized shape divergences. In both the above approaches, the representation scheme serves as a preprocessing for a clustering framework that would take over the detection of distinct signal sources (i.e. active neurons) and the isolation of the corresponding spiking contributions.

Regarding clustering, Bayesian [3] and Expectation Maximization [4] methods have been proposed for spike sorting. Assuming a stationary Gaussian profile for the background noise, both methods consider Gaussian properties for the potential clusters residing in the PCA representation subspace. However, in the general form, background noise in neural recordings is non-stationary, non-Gaussian and carries a complex correlated profile with higher power in low frequencies. Synaptic coupling among neurons, superimposed field potentials and bursting neurons are some of the reasons that would make a non-Gaussian cluster profile more plausible. To avoid Gaussian considerations, clustering approaches featuring hierarchical [5] and nearest-neighbors [2] algorithms have also appeared. The later employs a stochastic algorithm, known as super-paramagnetic clustering (SPC), which makes no prior assumptions for the statistical properties of the data.

There are two important parameters when one evaluates a spike sorting classification process: the number of clusters (i.e. active neurons) being decided by the process and the number of spikes assigned in each cluster. Both are well incorporated by Type I / II errors [4] in the spike sorting domain. Type I (false positive (FP)) / II (false negative (FN)) errors derive from the traditional classification schemes and conceptualize misclassification. For example, the identification of less neurons than expected (under-clustering) leads to high false positive errors, while the opposite case (over-clustering) results in a large amount of false negatives. Although a correct estimation of the number of clusters would limit both errors in cluster-delineation, the identification of actual number of active neurons is still an open issue. Even popular methods (like SPC) do not incorporate a sufficient treatment of this issue, leading to inappropriate results [6]. It is worth noting that, in laboratory practice, over-clustering is most often addressed in a less time-consuming way than under-clustering. In a previous work [1] we have stressed the importance of the previous fact and proposed a new cluster error definition that favors over-clustering over under-clustering errors.

P.D. Bamidis and N. Pallikarakis (Eds.): MEDICON 2010, IFMBE Proceedings 29, pp. 5–8, 2010.
www.springerlink.com

There are two main reasons why the identification of neurons' number is still an open issue. The first relates to the adopted clustering techniques, which require the a priori definition of number of groups. The second relates to the low SNR of the signals and the subsequent poor representation (in the original or reduced space) of the waveforms.

In this work, we propose a sequential, subtractive clustering algorithm which is based on graph theoretic ideas and in particular the notion of dominant set [7]. The algorithm works in an iterative fashion by operating on a neighborhood graph. It identifies the core of the graph, using replicator dynamics formulation, and then removes it from the graph and feeds back the remaining graph. The procedure terminates when all the data have been assigned to distinct groups or no more compact group can be formed any further. The suggested algorithm is engaged to work within a representation space which is derived via a fully compatible dimensionality reduction technique, namely Isometric feature mapping (ISOMAP) [8]. ISOMAP is known to reveal the intrinsic data variation and is therefore expected to be insensitive to random variations due to noise. Hence, the resulting low-dimensional parameterization of the waveform variation is expected to enhance the clustering performance.

Section II describes the proposed methodology. Section III presents the comparative evaluation of our spike sorting technique in relation with a popular alternative [2], using simulated data. Section IV concludes the paper.

II. METHOD

A. Low-dimensional Representation

The segments, extracted from the time-series of extracellular recordings via a root-mean-square threshold detector, are considered as the first raw representation of spiking activity. The ensemble of these loosely aligned spike-waveforms can be thought as a point-swarm residing in a multidimensional feature space with axes corresponding to signal amplitudes at particular latencies. Following the standard convention, the i^{th} spike waveform is depicted as $x_i(t)$, t=1,2,…,T, i=1,2,…,N (with *t* denoting discrete time or latency) and represented via the row-vector $\boldsymbol{x_i} = [x_i(1), x_i(2),\ldots, x_i(t),\ldots, x_i(T)] \in R^T$. Similarly the whole ensemble is represented in a data-matrix format as $\boldsymbol{X}_{[N\,x\,T]} = [\mathbf{x_1} \mid \mathbf{x_2} \mid \ldots \mathbf{x_i} \mid \ldots \mathbf{x_N}]$.

Most often an enhanced representation is sought by employing a dimensionality reduction technique (denoising step). Here, we employ ISOMAP embedding in order to achieve a parsimonious representation, in which the true degrees of freedom can be easily recognized and directly associated with involved neurons.

The algorithmic details of ISOMAP technique can be found elsewhere [9]. It starts by building a neighborhood graph over the data-points in the original feature space. This graph is then used to compute all the geodesic inter-point distances. Multidimensional scaling is finally employed to derive a reduced coordinate space where these distances are preserved and therefore the intrinsic geometry of the data is faithfully represented. In our case, the ISOMAP-routine provides a geometrical picture, within an *r*-D space, of the spike-waveforms variation.

$$\mathbf{Y}_{[N\,x\,r]} = [\mathbf{y_1} \mid \mathbf{y_2} \mid \ldots \mathbf{y_i} \mid \ldots \mathbf{y_N}] = \text{ISOMAP}(\mathbf{X}, r) \quad (1),$$

where $\mathbf{y_i} = [\, y_i(1), y_i(2),\ldots, y_i(r)\,] \in R^r$.

The derived point-swarm (for a 2-d example, see Figure 1b) is accompanied with the *residual variance*, which is a performance index ranging from 0% to 100% and indicating the reliability of the mapping (for an example, see Figure 1c). The optimal dimensionality r_o can be sought (as a compromise between accuracy and compression) by computing multiple maps with increasing *r* ($r \in [1,10]$), drawing the diagram of *residual variance* as a function of *r* and applying the '*elbow rule*'.

B. Identifying neurons and classifying the data

A recently introduced graph-theoretic algorithm [7] was employed for identifying the most-cohesive groups of vertices given the weighted similarity (adjacency) matrix of a graph. The algorithm is based on the identification of the dominant set of nodes and when repeatedly applied facilitates the effective clustering, in a sequential mode, of pairwise relational data. As stated in [7], the main property of a dominant set is that the overall similarity among internal nodes is higher than that between external and internal nodes, and this fact is the motivation of considering a dominant set as a cluster of nodes.

One of its main characteristics is the compact, elegant formulation. In our case, ISOMAP-representation points ($\boldsymbol{Y}$) are used to build an undirected edge-weighted graph with no self-loops $G=(V, E, w)$, where $V = \{1,\ldots, N\}$ is the vertex set, $E \subseteq V \times V$ is the edge set and $w : E \rightarrow R_+^*$ is the positive weight function. Vertices represent data points, edges correspond to neighborhood relationships and edge-weights reflect similarity between pairs of linked vertices.

In a preprocessing step, Euclidean distances d_{ij} are transformed to similarity weights, which increase with decreasing distances. For this transformation, we use the following form:

$$w(i, j) = \exp(-d_{ij} / \sigma) \quad (2),$$

where σ is a real positive number estimated as 3 times the average of the mean distance of all d_{ij}. Consequently, we

represent the N-node graph *G (V, E, w)* with the corresponding similarity matrix A, with *i* representing the *i*-th data point and the weight of edge *(i, j)* being set to *w(i,j): A =(a_{ij})* where $\alpha_{ij} = w(i, j)$ if $(i, j) \in E$ and $\alpha_{ij} = 0$ otherwise.

As pointed in [7], the cohesiveness of a cluster is measured by the overall similarity of a dominant set; that is, a good cluster contains elements that have large values connecting one another in the similarity matrix. Hence, the problem of finding a compact cluster is formulated as the problem of finding a vector x that maximizes the following objective function:

$$f(x) = x^T A\, x \qquad (3),$$

subject to $x \in \Delta$, where $\Delta=\{x\in R^n : x \geq 0 \text{ and } e^T x = 1\}$.

Thus, a maximally cohesive cluster denotes the most dominant solution set that is iteratively subtracted from the N-node graph (G). At the end of the iterations, where all the data have been classified, the overall cohesiveness *f(x)* of each step is exploited for the decision about the actual number of active neurons (for an example, see Figure 1d).

III. Results

For the detailed evaluation of our method, we generated spike waveforms representing neural activity from three separate neurons. Aiming at realistic simulations, we utilized real action potentials from respiratory motoneurons which had been recorded *in vitro* with a single "hook" electrode from the peripheral nervous system of the beetle Tenebrio molitor [10]. Three such action potential waveforms served as the initial templates. These waveforms were recorded extracellularly with a sampling frequency of 30 kHz and time duration of 4 ms (120 samples). The templates were replicated multiple times and added to segments of background noise extracted from the same recording (randomly extracted from latencies during which the spike-detector was silent). In order to pursue evaluation results under different SNR-levels, each extract of real background noise was modulated by a variable, positive amplitude factor ϕ. The SNR of the resulting waveform (template plus noise segment) was then defined as follows:

$$\text{SNR} = \frac{\text{RMS(template waveform)}}{\phi \cdot \text{RMS(random noise extract)}} \qquad (4)$$

Three hundreds (300) waveforms per template were generated yielding 900 single spikes corresponding to the three neural classes of our data set. In addition, paired combinations among the three templates were realized by first inducing variable delays and then adding noise segments

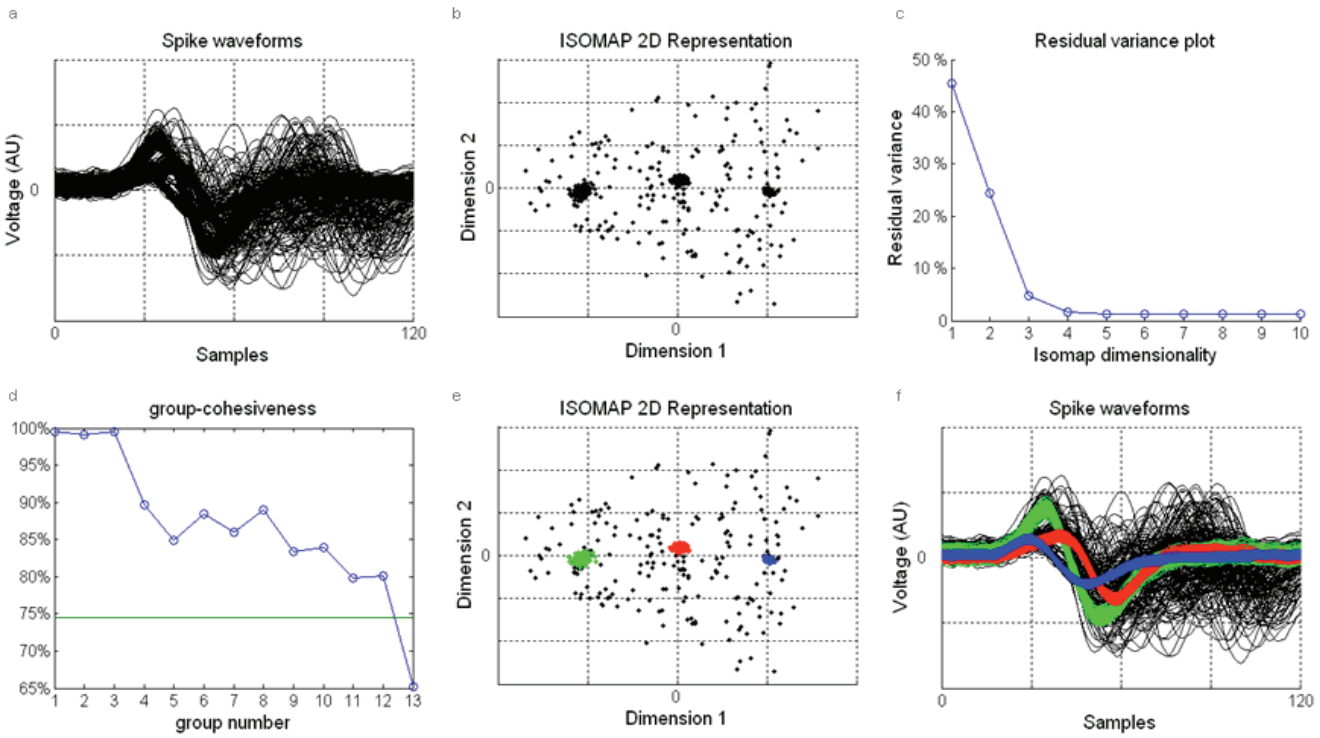

Figure 1: a) The overall simulated data set; The SNR is 5 for all waveforms. b) 2-D ISOMAP representation of the data set. c) Residual variance diagram of ISOMAP. The optimal dimensionality (r_o=4) is selected using the *elbow rule*. d) Group-cohesiveness values, iteratively computed for each subtracted cluster. e) Classification results visualized within 2-D ISOMAP space. Colors indicate classes, while unclassified data are left black. f) Classification results presented in the original data domain using the corresponding colors.

using amplitude factors so as to achieve a given SNR-level. In this way 150 waveforms of double-overlaps were generated; 50 for each template pair. Finally, 50 more waveforms were added corresponding to triple overlaps with their SNR-level adjusted accordingly. The complete data set of 1100 waveforms is shown in Figure 1a.

The 2-D ISOMAP representation of this dataset is shown in Figure 1b. Considering the high density areas of this point-diagram, there are apparently three clusters (pointing at the existence of three active neurons). The residual variance graph, which is a supplementary output of the ISOMAP routine, is included in Fig.1c and clearly designates the first four dimensions as necessary for the faithful low-dimensional representation of the data. Hence, the first four ISOMAP coordinates were used to represent each spike waveforms and dominant-set clustering was applied to the new data matrix $Y_{[1100 \text{ x } 4]}$. The overall cohesiveness for every cluster subtracted by the iterative process is shown in Figure 1d. The high ranking of the first three groups denotes the presence of three active neurons in the data. The straight line in the figure depicts the cluster quality for the whole graph taken as single component. For the selected groups, the classification algorithm assigns their waveforms to the corresponding classes, while the rest were left unclassified. This data-sieving procedure step is visualized in ISOMAP space (Figure 1e) and in the original data domain (Figure 1f) using a three-level color-code.

Type I/II errors were used for the performance evaluation. The total number of FP and FN is referred to the identified classes. The adopted *error-rate* accounts for the total number of false positive and false negative spikes:

$$\text{Error\_rate} = \frac{\sum_i \left(\text{Fp}_i + \text{Fn}_i \right)}{\text{Total \# of participating waveforms}} \cdot 100\% \qquad (5)$$

with i running over the number of single-spike classes (i.e. the number of identified neurons). For comparison purposes, the measurements corresponding to Waveclus [2] are also included. Both Waveclus and our proposed methodology classified the spikes of the data set into three main classes and an additional noise class. The results of this classification are shown in Figure 2, using 10 different realizations of the dataset. Averaged values for the error-rates and the FP-FN errors are shown as a function of SNR level. It can be seen that our proposed algorithm achieves the lowest error rate which is lower than 1% when the SNR is higher than 4.

CONCLUSIONS

The present work introduces a graph-theoretical approach to spike sorting; it iteratively pursuits a dominant set in the graph (the most dominant in each iteration) and then removes it, until all the data have been clustered. The efficiency of the proposed clustering method has been combined with the robustness of ISOMAP representation. The hybrid scheme has been extensively evaluated. The results indicate high robustness to noise and a measured performance that goes beyond the contemporary standards.

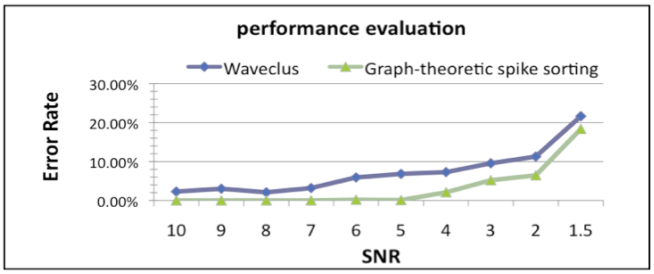

Figure 2: Average error rates for our method and Waveclus.

REFERENCES

1. Adamos DA, Kosmidis EK and Theophilidis G. (2008) Performance evaluation of PCA-based spike sorting algorithms. Computer methods and programs in biomedicine 91(3):232-44
2. Quian Quiroga R, Nadasdy Z, Ben-Shaul Y (2004) Unsupervised Spike Detection and Sorting with Wavelets and Superparamagnetic Clustering. Neural Comp 16:1661-1687.
3. Lewicki M (1998) A review of methods for spike sorting: the detection and classification of neural action potentials. Network: Computation in Neural Systems 9:R53-R78.
4. Harris KD, Henze DA, Csicsvari J, Hirase H, Buzsaki G (2000) Accuracy of Tetrode Spike Separation as Determined by Simultaneous Intracellular and Extracellular Measurements. J Neurophysiol 84:401-414.
5. Fee MS, Mitra PP, Kleinfeld D (1996) Automatic sorting of multiple unit neuronal signals in the presence of anisotropic and non-Gaussian variability. Journal of Neuroscience Methods 69:175-188.
6. Herbst JA, Gammeter S, Ferrero D, Hahnloser RH (2008) Spike sorting with hidden Markov models. J Neurosci Methods 174 (1):126-34
7. Pavan M and Pelillo M (2007) Dominant Sets and Pairwise Clustering. IEEE Trans. Pattern Anal. Mach. Intell. 29(1): 167-172
8. Tenenbaum JB, de Silva V, Langford JC (2000) A global geometric framework for nonlinear dimensionality reduction. Science 290(5500):2319-23
9. Laskaris NA and Ioannides AA (2002) Semantic geodesic maps: a unifying geometrical approach for studying the structure and dynamics of single trial evoked responses. Clinical Neurophysiology 113(8):1209-1226
10. Zafeiridou G and Theophilidis G (2004) The action of the insecticide imidacloprid on the respiratory rhythm of an insect: the beetle Tenebrio molitor. Neuroscience Letters 365(3):205-209

Author: Dimitrios A. Adamos
Institute: School of Biology, Aristotle University
Street: Aristotle University Campus, 54124
City: Thessaloniki
Country: Greece
Email: dadam@bio.auth.gr